



Scholars Research Library

Der Pharma Chemica, 2015, 7(3):125-141
(<http://derpharmachemica.com/archive.html>)



ISSN 0975-413X
CODEN (USA): PCHHAX

2H-indeine-1,3-dione derivatives as corrosion inhibitors for C-steel- theoretical and experimental study

A. S. Fouda^{1*}, H. A. Etman¹, A. El-Desoky², H. Abd El Aziz³ and A. M. Metwally³

¹Chemistry Department, Faculty of Science, El-Mansoura University, El-Mansoura, Egypt

²Engineering Chemistry Department, High Institute of Engineering & Technology (New Damietta), Egypt and Al-Qunfudah Center for Scientific Research (QCSR), Al-Qunfudah University College, Umm Al-Qura University, KSA

³Egyptian Natural Gas Company (GASCO), Talkha - Shirbin High Way, Talkha, Egypt

ABSTRACT

The influence of 2H-indeine-1, 3-dione derivatives on C- steel corrosion was studied in 1 M HCl solutions at 30°C. Measurements were conducted using weight loss, potentiodynamic polarization, electrochemical impedance spectroscopy (EIS) and electrochemical frequency modulation (EFM) techniques. These studies have shown that 2H-indeine-1, 3-dione derivatives are mixed-type inhibitors. Corrosion rates obtained from both EFM and EIS methods are comparable with those recorded using Tafel extrapolation method, confirming validation of corrosion rates measured by the latter. The inhibitive action of these 2H-indeine-1, 3-dione derivatives was discussed in terms of blocking the electrode surface by adsorption of the molecules through the active centers contained in their structures following Temkin adsorption isotherm. Quantum chemical method was also employed to explore the relationship between the inhibitor molecular properties and its protection efficiency. The morphology of inhibited and uninhibited C- steel was analyzed by scanning electron microscope (SEM) and energy dispersive X-ray spectroscopy (EDX).

Keywords: 2H-indeine-1, 3-dione derivatives, C- steel, HCl, EFM, EIS, SEM-EDX.

INTRODUCTION

C-steel has been extensively used under different conditions in petroleum industries^[1]. Aqueous solutions of acids are among the most corrosive media and are widely used in industries for pickling, acid cleaning of boilers, descaling and oil well^[2, 6]. The main problem concerning C- steel applications is its relatively low corrosion resistance in acidic solution. Several methods used currently to reduce corrosion of C- steel. One of such methods is the use of organic inhibitors^[7- 17]. Effective inhibitors are heterocyclic compounds that have π bonds, heteroatoms such as sulphur, oxygen and nitrogen^[18]. Compounds containing both nitrogen and chloro atoms can provide excellent inhibition, compared with compounds containing only nitrogen or chloro atom^[19]. Heterocyclic compounds such as 2H-indeine-1, 3-dione derivatives can provide excellent inhibition. These molecules depends mainly on certain physical properties of the inhibitor molecules such as functional groups, steric factors, electron density at the donor atom and electronic structure of the molecules^[20, 21]. Regarding the adsorption of the inhibitor on the metal surface, two types of interactions are responsible. One is physical adsorption which involves electrostatic force between ionic charges or dipoles of the adsorbed species and electric charge at metal/ solution interface. Other is chemical adsorption, which involves charge sharing or charge transfer from inhibitor molecules to

the metal surface to form coordinated types of bonds ^[22]. The selection of appropriate inhibitors mainly depends on the type of acid, its concentration, and temperature.

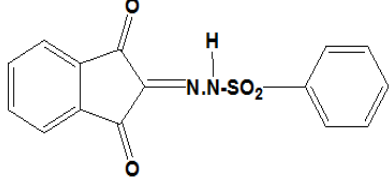
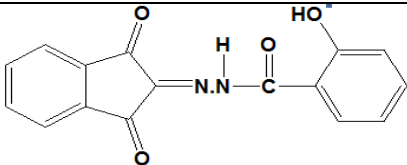
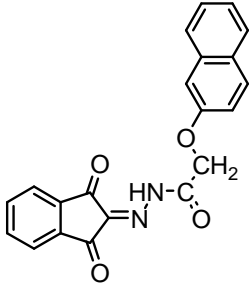
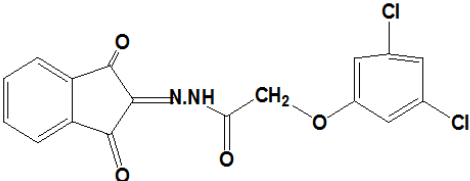
The objective of the present investigation is to study the corrosion inhibition of C- steel in 1 M HCl using 2H-indeine-1,3-dione derivatives by different techniques and to propose a suitable mechanism for the inhibition process. The surface morphology of carbon steel was examined using scanning electron microscopy (SEM) and energy dispersive X-ray (EDX).

MATERIALS AND METHODS

2.1. Chemicals and materials

Hydrochloric acid (37%), ethyl alcohol was purchased from Al-Gomhoria Company. Bidistilled water was used throughout all the experiments. 2H-indeine-1, 3-dione derivatives were prepared and characterized as before ^[22] (Table 1).

Table (1): Molecular structures, formulas and molecular weights of the investigated 2H-indeine-1, 3-dione derivatives

Comp.	Structures	Names	Mol. Formulas and Mol. Weights
1		2- benzenesulfonyl-hydrazone-2H-indene-1,3-dione	C ₁₅ H ₁₀ N ₂ O ₄ S 314
2		2-hydroxybenzohydrazone-2H-indene-1,3-dione	C ₁₆ H ₁₀ N ₂ O ₄ 294
3		2-(naphthalene-2-yloxy)-aceto hydrazone-2H-indeine-1,3-dione	C ₂₁ H ₁₄ N ₂ O ₄ 358
4		2-(3,5-dichlorophenoxy)-acetohydrazone-2H-indene-1,3-dione	C ₁₇ H ₁₀ N ₂ O ₄ Cl ₂ 377

The composition of C- steel (weight %) is given in Table (2) :

Table (2): Chemical composition of C- steel (weight %)

Element	C	Mn	P	Si	Fe
Weight (%)	0.200	0.350	0.024	0.003	rest

2.2. Methods

2.2.1. Weight loss measurements

Rectangular specimens of C-steel with dimensions 2.1 x 2.0 x 0.2 cm were abraded with different grades of emery papers, degreased with acetone, rinsed with bidistilled water and dried between filter papers. After weighting accurately, the specimens were immersed in 100 ml of 1 M HCl with and without different concentrations of inhibitors at 30°C. After different immersion periods, the C-steel samples were taken out, washed with bidistilled water, dried and weighted again. The weight loss values are used to calculate the corrosion rate (R) in mm^{-1} by Eq. (1):

$$R = (\text{weight loss in gram} \times 8.75 \times 10^4) / \text{DAT} \quad (1)$$

Where D is C- steel density in g cm^{-3} , A is exposed area in cm^2 ; T is exposure time in hr.

The inhibition efficiency (%IE) and the degree of surface coverage (θ) were calculated from Eq. (2):

$$\% \text{ IE} = \theta \times 100 = [(R^* - R) / R^*] \times 100 \quad (2)$$

Where R^* and R are the corrosion rates of C- steel in the absence and in the presence of inhibitor, respectively.

2.2.2. Electrochemical measurements

Electrochemical measurements were conducted in a conventional three electrodes thermostated cell assembly using Gamry Potentiostat/Galvanostat/ZRA (model PCI300/4). A platinum foil and saturated calomel electrode (SCE) were used as counter and reference electrodes, respectively. The C- steel electrodes were 1x1 cm and were welded from one side to a copper wire used for electrical connection. The electrodes were abraded, degreased and rinsed as described in weight loss measurements. The potentiodynamic curves were recorded from -500 to 500 mV at a scan rate 1 mV s^{-1} after the steady state is reached (30 min) and the open circuit potential (OCP) was noted. The % IE and degree of surface coverage were calculated from Eq. (3):

$$\% \text{ IE} = \theta \times 100 = [1 - (i_{\text{corr}}^0 / i_{\text{corr}})] \times 100 \quad (3)$$

Where i_{corr}^0 and i_{corr} are the corrosion current densities of uninhibited and inhibited solution, respectively.

Electrochemical impedance spectroscopy (EIS) and electrochemical frequency modulation (EFM) experiments were carried out using the same instrument as before with a Gamry framework system based on ESA400. Gamry applications include software EIS300 for EIS measurements and EFM140 for EFM measurements; computer was used for collecting data. Echem Analyst 5.5 Software was used for plotting, graphing and fitting data. EIS measurements were carried out in a frequency range of 100 kHz to 10 mHz with amplitude of 5 mV peak-to-peak using ac signals at respective corrosion potential. EFM carried out using two frequencies 2 and 5 Hz. The base frequency was 1 Hz. In this study, we use a perturbation signal with amplitude of 10 mV for both perturbation frequencies of 2 and 5 Hz.

2. 2. 3. Surface morphology

The C-steel surface was prepared by keeping the specimens for 3 days immersion in 1 M HCl in the presence and absence of optimum concentrations of investigated derivatives, after abraded using different grades of emery papers up to 1200 grit size. Then, after this immersion time, the specimens were washed gently with bidistilled water, carefully dried and mounted into the spectrometer without any further treatment. The corroded C-steel surfaces were examined using scanning electron microscope (SEM) and X-ray diffractometer Philips (pw-1390) with Cu-tube (Cu $K\alpha_1$, $\lambda = 1.54051 \text{ \AA}$), a scanning electron microscope (SEM, JOEL, JSM-T20, Japan).

2. 2.4. Theoretical study

Accelrys (Material Studio Version 4.4) software for quantum chemical calculations has been used.

RESULTS AND DISCUSSION

3.1. Weight loss measurements

Figure (1) shows the weight loss–time curves for the corrosion of C-steel in 1 M HCl in the absence and presence of different concentrations of compound (1). Similar curves for other compounds were obtained and are not shown. The data of Table (3) show that, the inhibition efficiency increases with increase in inhibitor concentration from 3×10^{-6} to 18×10^{-6} M. The maximum inhibition efficiency was achieved at 18×10^{-6} M., therefore %IE tends to decrease in the following order:

Compound (1) > compound (2) and compound (3) > compound (4)

Table (3): Variation of inhibition efficiency (% IE) of different compounds with their molar concentrations from weight loss measurements at 120 min immersion in 1 M HCl at 30°C

Conc., (M)	inhibition efficiency (% IE)			
	1	2	3	4
3×10^{-6}	57.7	54.6	51.0	48.5
6×10^{-6}	62.5	59.4	56.3	52.3
9×10^{-6}	66.2	63.6	60.5	57.1
12×10^{-6}	70.0	67.9	65.3	62.4
15×10^{-6}	74.6	72.5	70.5	66.1
18×10^{-6}	81.5	78.4	74.8	70.3

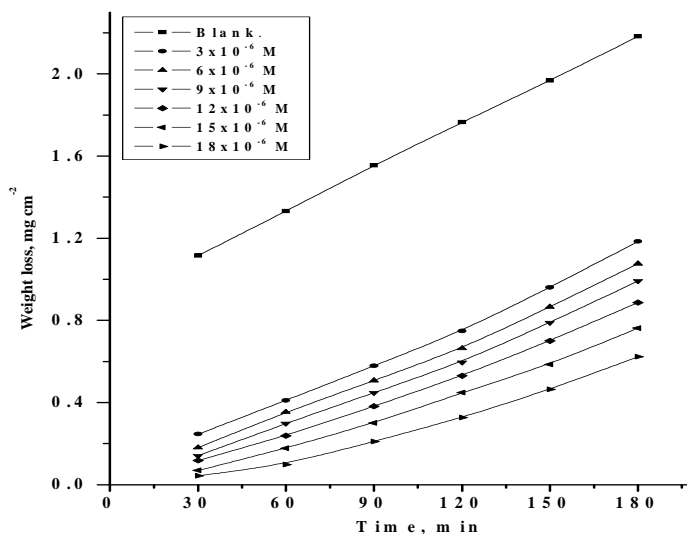


Figure (1): Weight loss-time curves for C- steel dissolution in 1 M HCl in the absence and presence of different concentrations of compound (1) at 30°C

3.1.2. Adsorption isotherms

Assuming the corrosion inhibition was caused by the adsorption of 2H-indeine-1, 3-dione derivatives, and the values of surface coverage for different concentrations of 2H-indeine-1, 3-dione derivatives in 1 M HCl were evaluated from weight loss. From the values of (Θ), it can be seen that these values increased with increasing the concentration of 2H-indeine-1, 3-dione derivatives. Using these values of surface coverage, one can utilize different adsorption isotherms to deal with experimental data. In this study, Temkin adsorption isotherm was found to be most suitable for the experimental findings. This isotherm is described by equation (4) as depicted from Figure (2).

$$2a\Theta = \ln (K_{ads} C) \quad (4)$$

Where C is the inhibitor concentration, K_{ads} is the adsorption equilibrium constant and 'a' is heterogeneous factor of metal surface. Equilibrium constant (K_{ads}) of adsorption process determined using (5) could be further used to determine free energy of adsorption (ΔG_{ads}°) as follows:

$$\Delta G_{ads}^{\circ} = -RT \ln (55.5 K_{ads}) \quad (5)$$

Where 55.5 is the concentration of water in the solution in M/L.

The thermodynamic parameters for the adsorption process that were obtained from the Figure is shown in Table (4). The values of ΔG_{ads}° are negative and increased as the % IE increased which indicate that these investigated 2H-indeine-1, 3-dione derivatives are strongly adsorbed on the C- steel surface and show the spontaneity of the adsorption process and stability of the adsorbed layer on the C-steel surface. Generally, values of ΔG_{ads}° up to - 20 kJ mol⁻¹ are consistent with the electrostatic interaction between the charged molecules and the charged metal (physical adsorption) while those more negative than - 40 kJ mol⁻¹ involve sharing or transfer of electrons from the inhibitor molecules to the metal surface to form a coordinate type of bond (chemisorptions)^[23]. The values of ΔG_{ads}° obtained were approximately equal to (61-58.2) kJ mol⁻¹, indicating that the adsorption mechanism of the 2H-indeine-1, 3-dione derivatives on C- steel in 1 M HCl solution involves both electrostatic adsorption and chemisorptions^[24,25]. The thermodynamic parameters point toward both physisorption (minor contributor) and chemisorptions (major contributor) of the inhibitors onto the metal surface. The K_{ads} follow the same trend in the sense that large values of K_{ads} imply better more efficient adsorption and hence better inhibition efficiency.

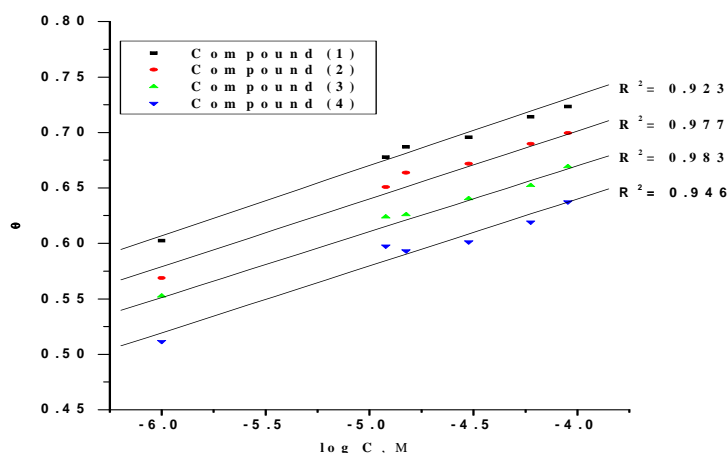


Figure (2): Curve fitting of corrosion data for C- steel in 1 M HCl in presence of different concentrations of 2H-indeine-1, 3-dione derivatives to the Temkin adsorption isotherm at 30°C

Table (4): Inhibitor binding constant (K), free energy of binding (ΔG_{ads}°) and later interaction parameter (a) for the organic derivatives for the corrosion of C-steel in 1 M HCl at 30°C

Inhibitors	Temkin		
	a	$K \times 10^{-8}$ mol L ⁻¹	$-\Delta G_{ads}^{\circ}$ kJ mol ⁻¹
Compound (1)	12.2	5.01	61.0
Compound (2)	12.0	3.88	59.4
Compound (3)	12.3	3.04	59.0
Compound (4)	12.1	2.02	58.2

3.1.3. Effect of temperature

The activation energies (E_a^*) for the corrosion of C- steel in the absence and presence of different concentrations of 2H-indeine-1,3-dione derivatives were calculated using Arrhenius-type Eq^[27]:

$$\log k = \log A - E_a^* / 2.303RT \quad (6)$$

Where A is the pre-exponential factor, k is the rate constant, E_a^* is the apparent activation energy of the corrosion process, R is the universal gas constant and T is the absolute temperature. Arrhenius plots of $\log k$ vs. $1/T$ for C-steel in 1 M HCl in the absence and presence of different concentrations of compound (1) are shown graphically in Figure (3). The variation of $\log k$ vs. $1/T$ is linear one and the values of E_a^* were calculated from the slope of these lines and given in Table (5). The increase in E_a^* with the addition of various concentrations of compounds (1-4) indicating that the energy barrier for the corrosion reaction increases. It is also indicated that the whole process is controlled by surface reaction, since the activation energy of the corrosion process is larger than 20 kJ mol^{-1} [27].

Enthalpy and entropy of activation (ΔH^* , ΔS^*) for the corrosion of C- steel in 1 M HCl were obtained by applying the transition state Eq. (7):

$$k = (RT/Nh) \exp(\Delta S^*/R) \exp(-\Delta H^*/RT) \quad (7)$$

Where h is Planck's constant, N is Avogadro's number. A plot of $\log k/T$ vs $1/T$ also gave straight lines as shown in Figure (4) for C- steel dissolution in 1 M HCl in the absence and presence of different concentrations of compound (1). The slopes of these lines equal $-\Delta H^*/2.303R$ and the intercept equal $\log RT/Nh + (\Delta S^*/2.303R)$ from which the value of ΔH^* and ΔS^* were calculated and tabulated in Table (5). From these results, it is clear that the presence of the tested compounds increased the activation energy values and consequently decreased the corrosion rate of the C-steel. These results indicate that these tested compounds acted as inhibitors through increasing activation energy of C-steel dissolution by making a barrier to mass and charge transfer by their adsorption on C-steel surface. Positive sign of the enthalpies reflects the endothermic nature of the C-steel dissolution process. All values of E_a^* are larger than the analogous values of ΔH^* indicating that the corrosion process must involved a gaseous reaction, simply the hydrogen evolution reaction, associated with a decrease in the total reaction volume [28]. The values of ΔS^* in the presence of the investigated compounds are large and negative; this indicates that the activated complex in the rate-determining step represents an association rather than dissociation step, meaning that a decrease in disordering takes place on going from reactants to the activated complex [29,30].

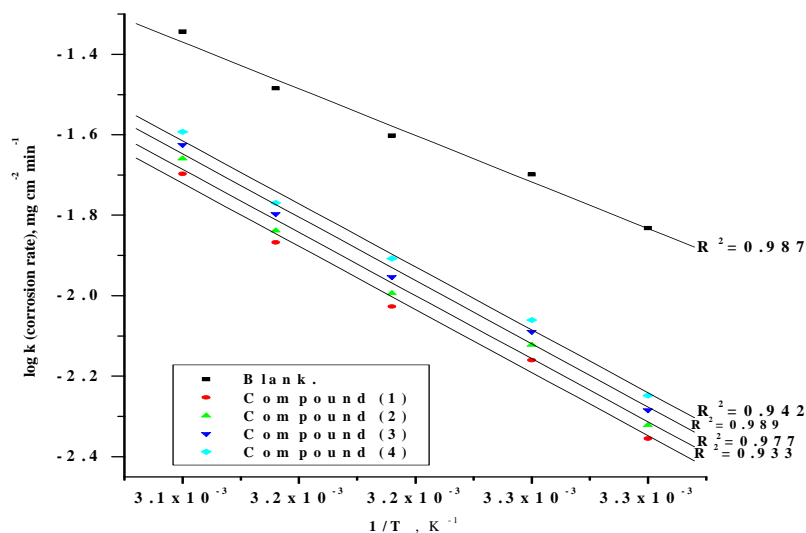


Figure (3): Arrhenius plots ($\log k$ vs $1/T$) for C-steel in 1 M HCl in absence and presence of different concentrations of compound (1)

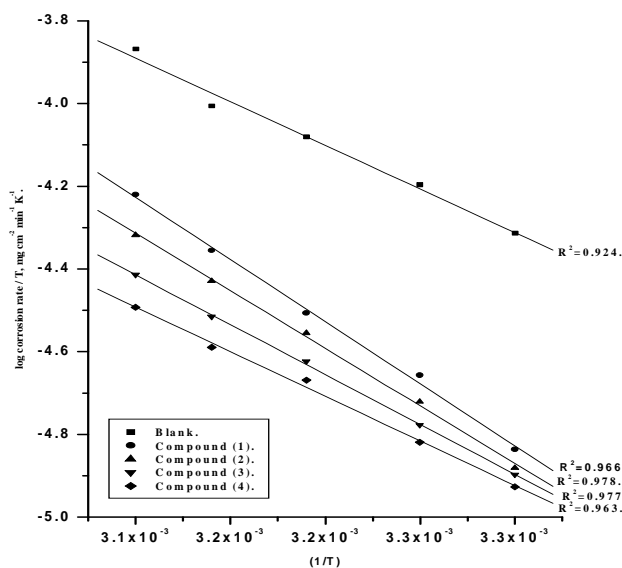


Figure (4): Transition state plots ($\log k/T$ vs $1/T$) for C-steel in 1 M HCl in absence and presence of different concentration of compound (1)

Table (5): Activation parameters of the dissolution of C-steel in 1 M HCl in the absence and presence of different concentrations of 2H-indeine-1,3-dione derivatives

Inhibitor	Activation Parameters		
	E_a^* kJ mol^{-1}	ΔH^* kJ mol^{-1}	$-\Delta S^*$ $\text{J mol}^{-1} \text{K}^{-1}$
Blank	45.4	42.9	143.5
Compound (1)	61.1	60.3	102.3
Compound (2)	59.3	58.9	100.8
Compound (3)	58.6	58.5	99.9
Compound (4)	54.4	53.8	95.7

3.2. Potentiodynamic polarization measurements

The cathodic and anodic polarization curves for C-steel in 1 M HCl solution in absence and presence of various concentrations of the compound (1) at 30 °C are shown in Figure.(5). Similar curves were obtained for other compounds (not shown). The various electrochemical parameters calculated from Tafel plots are given in Table (6). The lower corrosion current density (i_{corr}) values in presence of these compounds without causing significant changes in corrosion potential (E_{corr}) suggest that the investigated compounds are mixed type inhibitors and are adsorbed on the surface thereby blocking the corrosion reaction^[31]. The results show also that the slopes of the anodic and the cathodic Tafel slopes (β_a and β_c) were slightly changed on increasing the concentration of the investigated compounds. This indicates that there is no change in the mechanism of inhibition in presence and absence of inhibitors. The values of β_c are slightly higher than the values of β_a suggesting a cathodic action of the inhibitor. The higher values of Tafel slope can be attributed to surface kinetic process rather the diffusion-controlled process^[32].

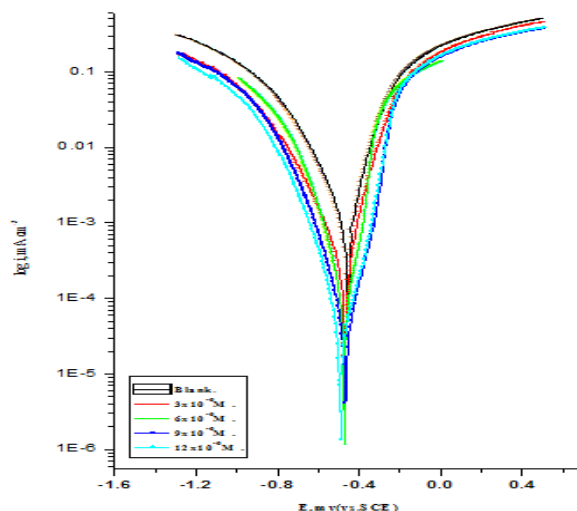


Figure (6): Potentiodynamic polarization curves for C-steel in 1 M HCl in the absence and presence of different concentrations of inhibitor (1) at 30°C

Table (6): The effect of concentration of the investigated compounds on the free corrosion potential (E_{corr}), corrosion current density (i_{corr}), Tafel slopes (β_a & β_c), inhibition efficiency (% IE), and degree of surface coverage for the corrosion of C-steel in 1 M HCl at 30°C

Concentration, M	i_{corr} , mA cm ⁻²	$-E_{\text{corr}}$, mV vs SCE	β_a , mV dec ⁻¹	β_c , mV dec ⁻¹	θ	% IE	
Blank	753.00	453	83.2	149.0	-	-	
(1)	3×10^{-6}	57.90	487	90.3	94.6	0.923	92.3
	6×10^{-6}	36.10	461	93.3	129.0	0.952	95.2
	9×10^{-6}	17.50	471	68.3	87.8	0.976	97.6
	12×10^{-6}	11.00	478	87.8	82.9	0.985	98.5
(2)	3×10^{-6}	211.00	470	80.3	141.0	0.719	71.9
	6×10^{-6}	89.00	473	95.3	96.3	0.881	88.1
	9×10^{-6}	40.20	467	107.0	98.7	0.946	94.6
	12×10^{-6}	31.90	492	117.0	87.0	0.957	95.7
(3)	3×10^{-6}	80.00	463	113.0	98.7	0.893	89.3
	6×10^{-6}	69.00	481	89.2	86.0	0.908	90.8
	9×10^{-6}	62.40	463	121.0	128.0	0.917	91.7
	12×10^{-6}	20.90	477	49.4	54.8	0.972	97.2
(4)	3×10^{-6}	717.00	453	84.8	151.0	0.047	4.70
	6×10^{-6}	696.00	454	95.3	141.0	0.075	7.50
	9×10^{-6}	106.00	437	85.0	91.4	0.859	85.9
	12×10^{-6}	455.00	455	47.0	62.0	0.940	94.0

3.3. Electrochemical impedance spectroscopy (EIS) measurements

The EIS provides important mechanistic and kinetic information for an electrochemical system under investigation. Figure (6) show the Nyquist plots for C-steel in 1 M HCl solution in the absence and presence of different concentrations of compound (1) at 30°C. Nyquist impedance plots exhibits a single semi-circle shifted along the real impedance (Z_r). The Nyquist plots of compound (1) do not yield perfect semicircles as expected from the theory of EIS, the impedance loops measured are depressed semi-circles with their centers below the real axis, where the kind of phenomenon is known as the “dispersing effect” as a result of frequency dispersion^[33] and mass transport resistant^[34] as well as electrode surface heterogeneity resulting from surface roughness, impurities, dislocations, grain boundaries, adsorption of inhibitors, formation of porous layers^[35-39], so one constant phase element (CPE) is substituted for the capacitive element, to explain the depression of the capacitance semi-circle, to give a more accurate fit. Impedance data are analyzed using the circuit in Figure (7); in which R_s represents the electrolyte resistance, R_{ct} represents the charge-transfer resistance and the constant phase element (CPE). According to Hsu and Mansfield^[40] the correction of capacity to its real values is calculated from Eq. (8):

$$C_{dl} = Y_o (\omega_{max})^{n-1} \tag{8}$$

Where Y_o is the CPE coefficient, ω_{max} is the frequency at which the imaginary part of impedance ($-Z_i$) has a maximum and n is the CPE exponent (phase shift).

The data obtained from fitted spectra are listed in Table (7). The %IE was calculated from Eq. (9):

$$\% IE = \left(1 - \frac{R_{ct}^o}{R_{ct}} \right) \times 100 \tag{9}$$

Where R_{ct} and R_{ct}^* are the charge-transfer resistances with and without the inhibitors, respectively.

Data in Table (7) Show that; the R_s values are very small compared to the R_{ct} values. Also; the R_{ct} values increase and the calculated C_{dl} values decrease by increasing the inhibitor concentrations, which causes an increase of θ and Y_1 . The high R_{ct} values are generally associated with slower corroding system [41]. The decrease in the C_{dl} suggests that inhibitors function by adsorption at the metal/solution interface [42]. The inhibition efficiencies, calculated from EIS results, show the same trend as those obtained from polarization measurements. The difference of inhibition efficiency from two methods may be attributed to the different surface status of the electrode in two measurements. EIS were performed at the rest potential, while in polarization measurements the electrode potential was polarized to high over potential, non-uniform current distributions, resulted from cell geometry, solution conductivity, counter and reference electrode placement, etc., will lead to the difference between the electrode area actually undergoing polarization and the total area [43].

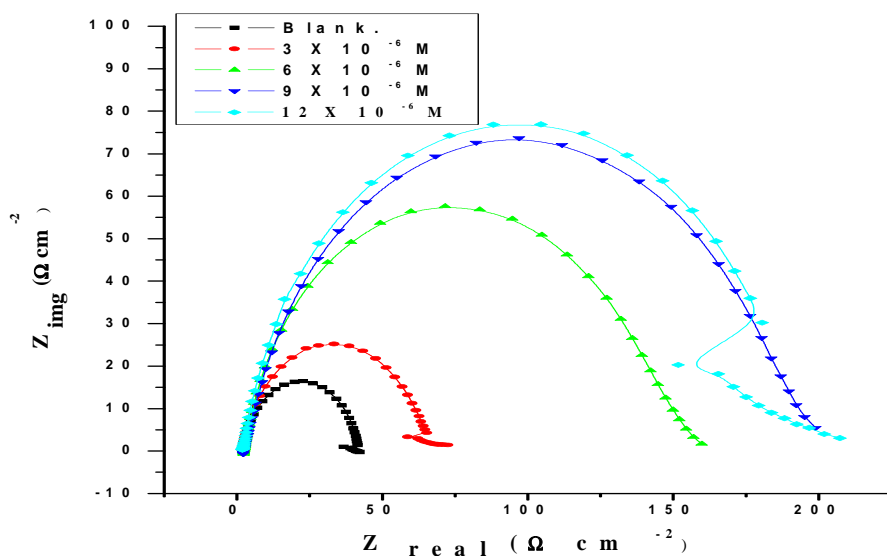


Figure (6): The Nyquist plots for corrosion of C-steel in 1 M HCl in the absence and presence of different concentrations of compound (1) at 30°C

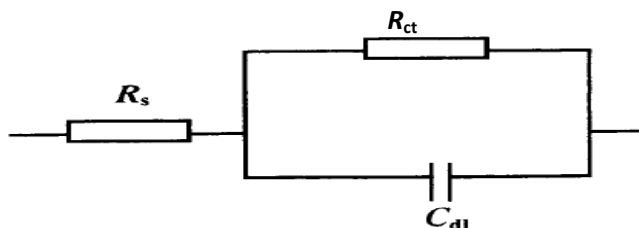


Figure (7): The equivalent circuit model used to fit the experimental results

Table (7): Electrochemical kinetic parameters obtained by EIS technique for in 1 M HCl without and with various concentrations of compounds at 30°C

Inhibitor	[inh] M	R_{ct} , $\Omega \text{ cm}^2$	C_{dl} , $\times 10^{-4}$ $\mu\text{F cm}^2$	Θ	% IE
Blank	0.0	40.38	2.00	-----	-----
(1)	3×10^{-6}	212.80	2.93	0.810	81.0
	6×10^{-6}	233.40	2.48	0.826	82.6
	9×10^{-6}	245.60	2.21	0.835	83.5
	12×10^{-6}	298.70	1.13	0.864	86.4
(2)	3×10^{-6}	64.90	4.76	0.377	37.7
	6×10^{-6}	149.00	3.95	0.728	72.8
	9×10^{-6}	195.40	1.94	0.793	79.3
	12×10^{-6}	197.60	1.82	0.795	79.5
(3)	3×10^{-6}	152.40	4.25	0.735	73.5
	6×10^{-6}	192.50	3.53	0.790	79.0
	9×10^{-6}	205.70	3.41	0.803	80.3
	12×10^{-6}	248.50	4.05	0.837	83.7
(4)	3×10^{-6}	74.92	6.79	0.461	46.1
	6×10^{-6}	90.49	6.68	0.553	55.3
	9×10^{-6}	110.10	8.63	0.633	63.3
	12×10^{-6}	154.10	3.58	0.737	73.7

3.4. Electrochemical frequency modulation measurements

Recently electrochemical frequency modulation (EFM) was used as a new electrochemical technique for online corrosion monitoring [41, 44-46]. EFM is a rapid and nondestructive corrosion rate measurement technique that can directly give values of the corrosion current without prior knowledge of Tafel constants. In corrosion research, it is known that the corrosion process is non-linear in nature, a potential distortion by one or more sine waves will generate responses at more frequencies than the frequencies of applied signal. Virtually no attention has been given to the intermodulation or electrochemical frequency modulation. However, EFM showed that this non-linear response contains enough information about the corroding system so that the corrosion current can be calculated directly. The great strength of the EFM is the causality factors which serve as an internal check on the validity of the EFM measurement. With the causality factors the experimental EFM data can be verified.

Figure (8) show the current response contains not only the input frequencies, but also contains frequency components which are the sum, difference, and multiples of the two input frequencies.

The electrochemical corrosion kinetic parameters at different concentrations of inhibitors in 1 M HCl at 30°C were shown in Table (8). The inhibition efficiency was found to increase with increasing the inhibitor concentrations. The causality factors CF-2 and CF-3 in Table (8) are close to their theoretical values of 2.0 and 3.0, respectively indicating that the measured data are of good quality.

The calculated inhibition efficiency obtained from weight loss, Tafel polarization and EIS measurements are in good agreement with that obtained from EFM measurements. Therefore %IE tends to decrease in the following order: compound (1) > compound (2) and compound (3) > compound (4)

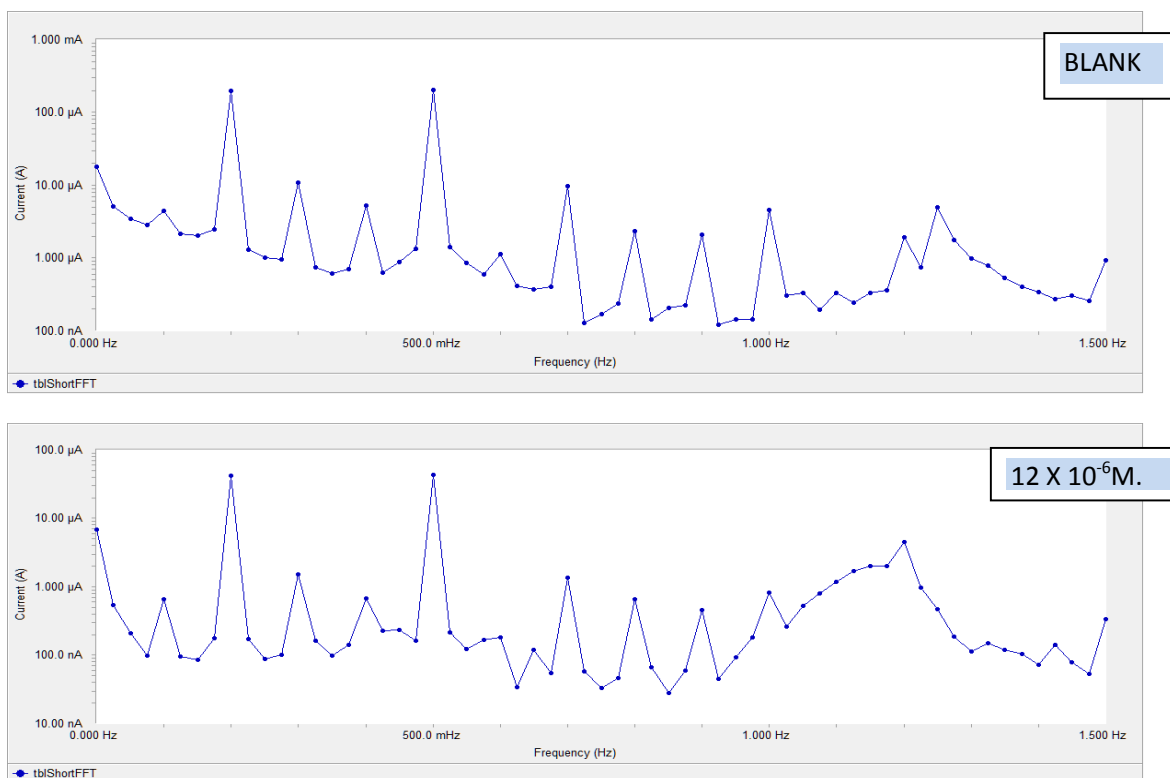


Figure (8): EFM spectra for C- steel in 1 M HCl in the absence and presence of 12×10^{-6} M of compound (1) at 30°C

Table (8): Electrochemical kinetic parameters obtained by EFM technique for C- steel in the absence and presence of various concentrations of investigated compounds in 1M HCl at 30°C

Comp.	Conc., M	i_{corr} $\mu\text{A cm}^{-2}$	β_c mV dec^{-1}	β_a mVdec^{-1}	CF-2	CF-3	CR	θ	% IE
(1)	Blank	470.1	88.4	94.3	1.91	3.50	214.8	----	----
	3×10^{-6}	93.77	95.9	101.0	2.32	2.81	42.85	0.800	80.0
	6×10^{-6}	87.75	95.0	100.0	1.99	2.99	40.09	0.813	81.3
	9×10^{-6}	57.56	107.0	115.0	1.92	2.74	26.30	0.877	87.7
	12×10^{-6}	38.7	79.0	86.0	1.81	2.83	17.68	0.917	91.7
(2)	3×10^{-6}	152.97	95.9	100.5	1.94	2.81	72.50	0.674	67.4
	6×10^{-6}	132.60	91.2	103.3	2.10	3.22	60.58	0.717	71.7
	9×10^{-6}	111.70	102.7	107.8	2.46	2.94	51.03	0.762	76.2
	12×10^{-6}	40.04	57.2	64.8	1.90	3.02	18.30	0.914	91.4
(3)	3×10^{-6}	158.20	114.0	132.0	1.95	3.09	72.28	0.663	66.3
	6×10^{-6}	114.30	111.0	124.0	1.72	3.40	52.24	0.756	75.6
	9×10^{-6}	72.98	94.5	160.0	2.00	2.52	33.35	0.844	84.4
	12×10^{-6}	62.38	66.3	68.1	2.03	2.88	28.50	0.867	86.7
(4)	3×10^{-6}	317.70	37.4	40.7	1.59	2.80	145.20	0.324	32.4
	6×10^{-6}	300.00	35.7	36.8	2.02	2.98	137.30	0.361	36.1
	9×10^{-6}	206.10	80.1	86.9	1.87	3.08	94.18	0.561	56.1
	12×10^{-6}	131.40	83.1	97.8	1.80	3.31	60.05	0.720	72.0

3.5- Scanning electron microscopy (SEM) studies

Figure (9) represents the micrograph obtained for C-steel samples in presence and in absence of 18×10^{-6} M of 2H-indeine-1, 3-dione derivatives after exposure for 3 days immersion. It is clear that C-steel surfaces suffer from severe corrosion attack in the blank sample. It is important to stress out that when the compound is present in the solution, the morphology of C-steel surfaces is quite different from the previous one, and the specimen surfaces were smoother. We noted the formation of a film which is distributed in a random way on the whole surface of the C-steel. This may be interpreted as due to the adsorption of the 2H-indeine-1, 3-dione derivatives on the C-steel surface incorporating into the passive film in order to block the active site present on the C-steel surface.

the involvement of inhibitor molecules in the interaction with the reaction sites of C-steel surface, resulting in a decrease in the contact between C-steel and the aggressive medium and sequentially exhibited excellent inhibition effect^[47, 48].

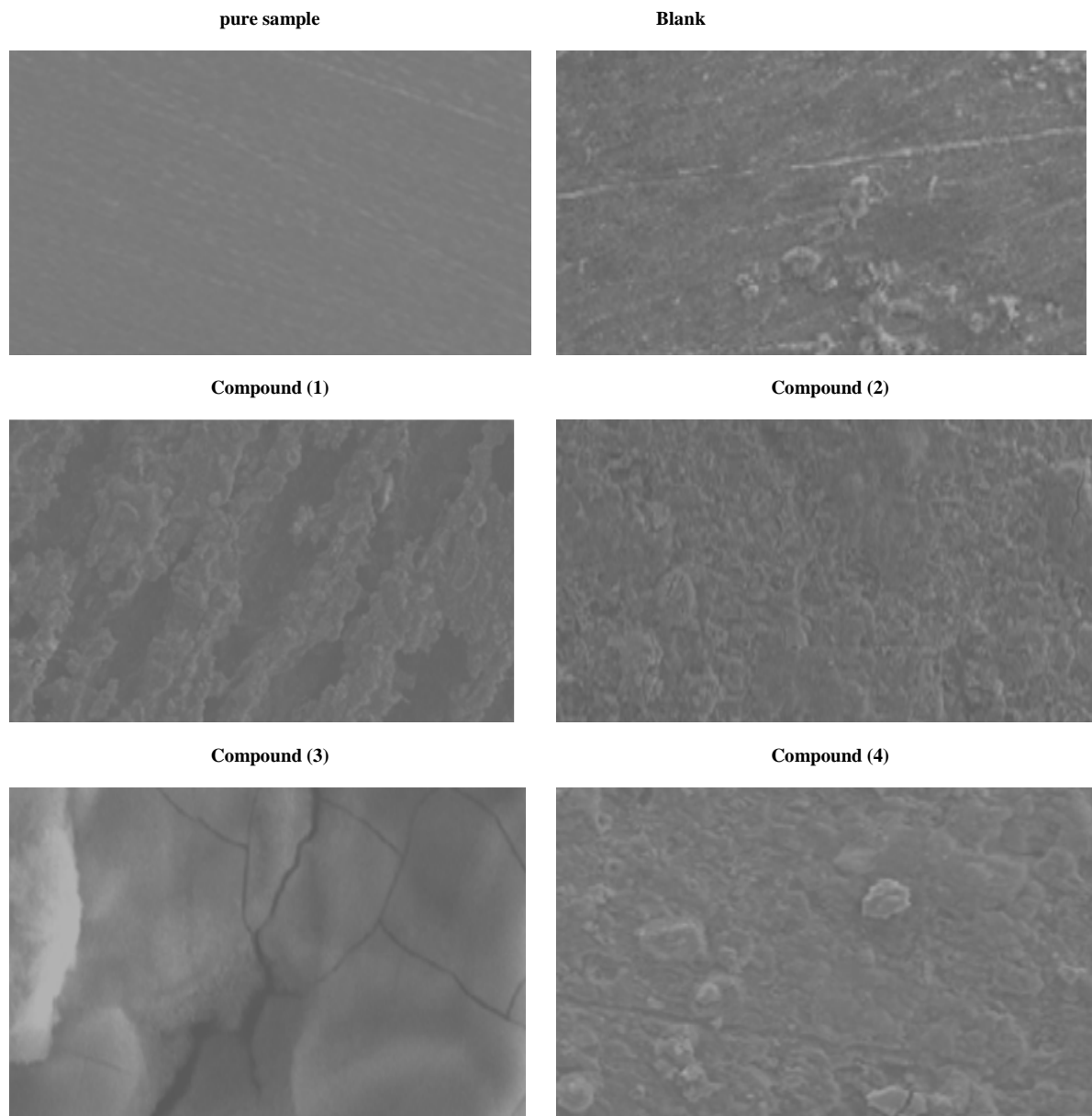


Figure (9): SEM images of C-steel in 1 M HCl solution after immersion for 3 days without inhibitor and in presence of 18×10^{-6} M of 2H-indeine-1,3-dione derivatives

3.6. Energy dispersion spectroscopy (EDX) studies

The EDX spectra were used to determine the elements present on the surface of C- steel and after 3 days of exposure in the uninhibited and inhibited 1 M HCl. Figure (10) shows the EDX analysis result on the composition of C- steel only without the acid and inhibitor treatment. The EDS analysis indicates that only Fe and oxygen were detected, which shows that the passive film contained only Fe_2O_3 . Figure (10) portrays the EDX analysis of C-steel in 1 M HCl only and in the presence of 18×10^{-6} M of 2H-indeine-1, 3-dione derivatives. The spectra show additional lines, demonstrating the existence of C (owing to the carbon atoms of 2H-indeine-1, 3-dione derivatives). These data

shows that the carbon and O atoms covered the specimen surface. This layer is entirely owing to the inhibitor, because the carbon and O signals are absent on the specimen surface exposed to uninhibited HCl. It is seen that, in addition to Mn, C. and O were present in the spectra. A comparable elemental distribution is shown in Table (9).

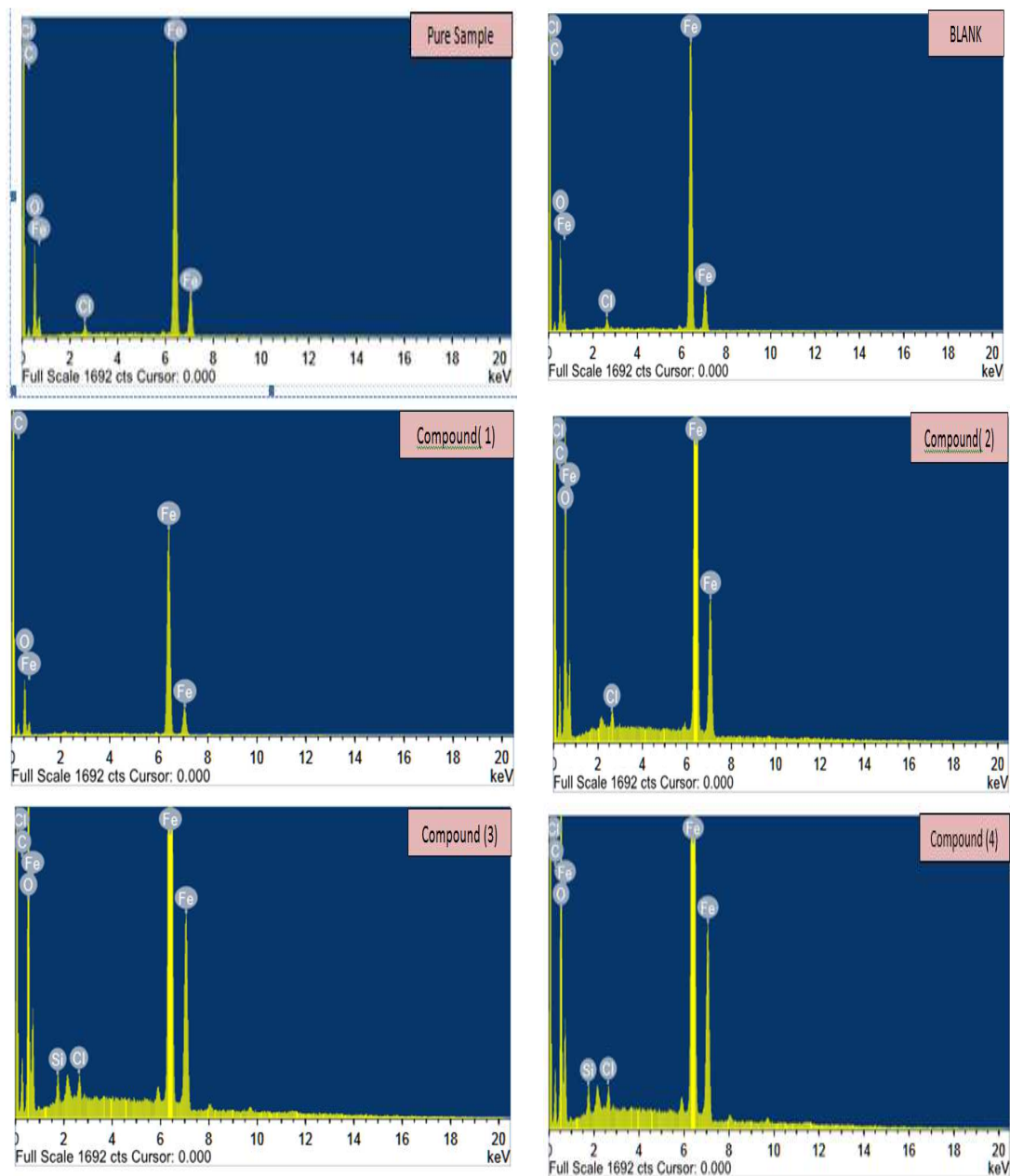


Figure (10): EDX analysis of C-steel in 1 M HCl solution after immersion for 3 days without inhibitor and in presence of 18×10^{-6} M of 2H-indeine-1,3-dione derivatives

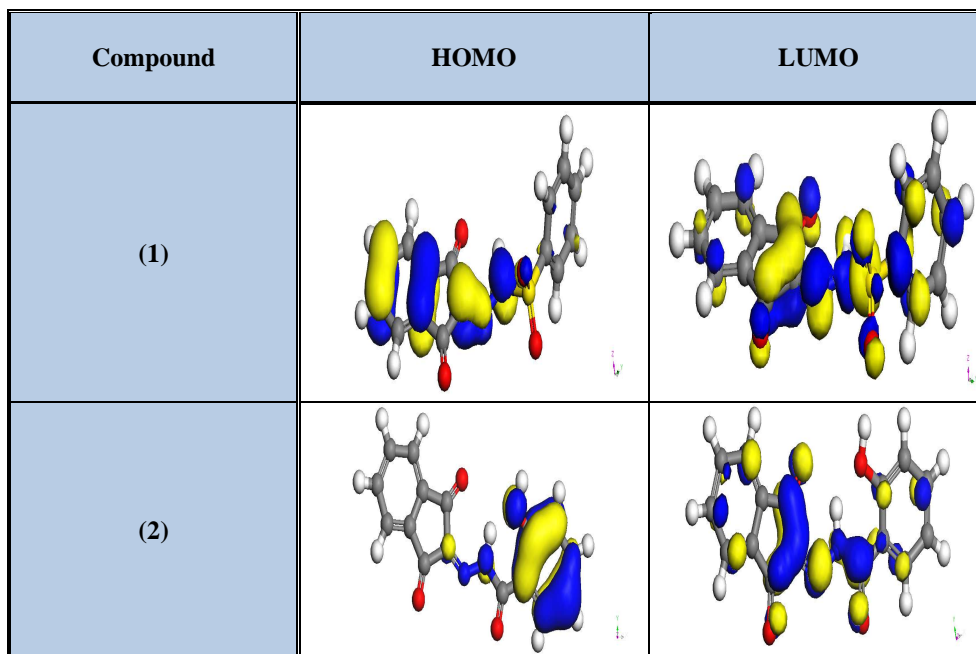
Table (9): Surface composition (weight %) of C-steel after 3hrs of immersion in HCl without and with the optimum concentrations of the studied inhibitors

(Mass %)	Fe	C	O	Cl	Si
Pure Sample	65.24	19.21	14.97	----	0.58
Blank	50.61	11.54	36.86	0.90	0.09
Compound (1)	54.57	22.61	21.87	0.50	0.45
Compound (2)	45.37	20.34	32.8	1.08	0.41
Compound (3)	54.71	17.14	27.08	0.50	0.57
Compound (4)	44.64	20.81	32.25	1.77	0.53

3.7. Quantum chemical calculations

Theoretical calculations were performed for only the neutral forms, in order to give further insight into the experimental results. Values of quantum chemical indices such as energies of LUMO and HOMO (E_{HOMO} and E_{LUMO}), and energy gap ΔE , are calculated by semi-empirical AM1, MNDO and PM3 methods has been given in Table (10). The reactive ability of the inhibitor is related to E_{HOMO} , E_{LUMO} ^[49]. Higher E_{HOMO} of the adsorbent leads to higher electron donating ability^[50]. Low E_{LUMO} indicates that the acceptor accepts electrons easily. The calculated quantum chemical indices (E_{HOMO} , E_{LUMO} , μ) of investigated compounds are shown in Table (10). The difference $\Delta E = E_{\text{LUMO}} - E_{\text{HOMO}}$ is the energy required to move an electron from HOMO to LUMO. Low ΔE facilitates adsorption of the molecule and thus will cause higher inhibition efficiency.

The bond gap energy ΔE increases from compounds (1 to 4). This fact explains the decreasing inhibition efficiency in this order ($1 > 2 > 3 > 4$), as shown in Table (10) and Figure (11) Show the optimized structures of the four investigated compounds. So, the calculated energy gaps show reasonably good correlation with the efficiency of corrosion inhibition. Table (10) also indicates that compound (1) possesses the lowest total energy that means that compound (1) adsorption occurs easily and is favored by the highest softness. The HOMO and LUMO electronic density distributions of these molecules were plotted in Figure (11). For the HOMO of the studied compounds that the benzene rings, N-atoms and O-atom have a large electron density. The data presented in Table (10) Show that the calculated dipole moment decrease from ($1 > 2 > 3 > 4$).



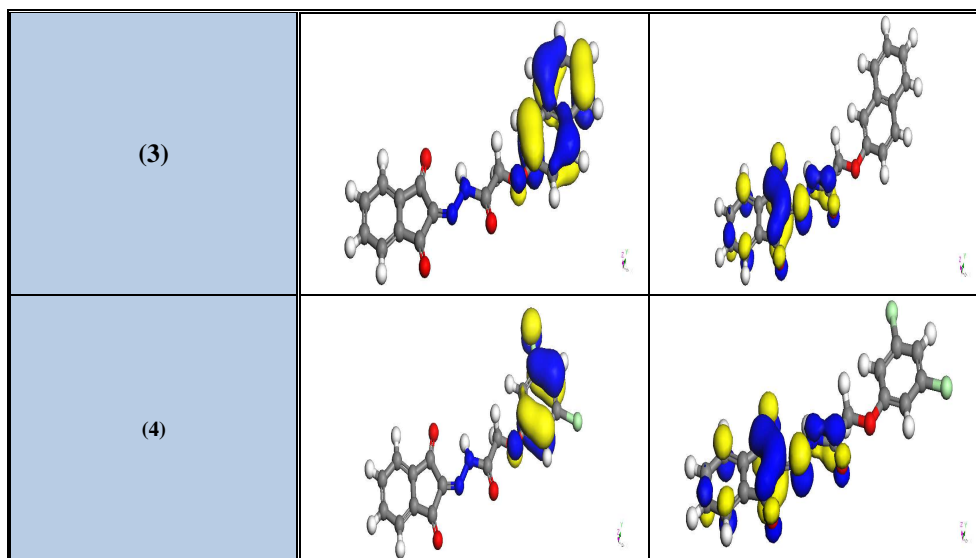


Figure (11): The Highest Occupied Molecular Orbital (HOMO) and the Lowest Unoccupied Molecular Orbital (LUMO) of the investigated compounds

Table (10): The calculated quantum chemical properties for investigated compounds

	Compound (1)	Compound (2)	Compound (3)	Compound (4)
$-E_{\text{HOMO}}$ (eV)	9.567	10.139	9.077	9.652
$-E_{\text{LUMO}}$ (eV)	1.345	1.266	1.241	1.244
ΔE (eV)	8.222	8.873	7.836	8.408
η (eV)	4.111	4.437	3.918	4.204
σ (eV ⁻¹)	0.243	0.225	0.255	0.238
$-\pi$ (eV)	5.456	5.703	5.159	5.448
χ (eV)	5.456	5.703	5.159	5.448
Dipole moment (Debye)	10.694	8.686	8.926	9.231

3.8. Mechanism of corrosion inhibition

Inhibition of the corrosion of C-steel in 1M HCl solution by some 2H-indeine-1,3-dione derivatives is determined by weight loss, potentiodynamic anodic polarization measurements, electrochemical impedance Spectroscopy (EIS) and electrochemical frequency modulation method (EFM). It was found that the inhibition efficiency depends on concentration, nature of metal, the mode of adsorption of the inhibitors and surface conditions. The observed corrosion data in presence of these compounds, namely: i) The decrease of corrosion rate and corrosion current with increase in concentration of the inhibitor ii) The linear variation of weight loss with time iii) The shift in Tafel lines to higher potential regions iv) The decrease in corrosion inhibition with increasing temperature indicates that desorption of the adsorbed inhibitor molecules takes place and v) The inhibition efficiency was shown to depend on the number of adsorption active centers in the molecule and their charge density. The corrosion inhibition is due to adsorption of these compounds at the electrode/ solution interface, the extent of adsorption of an inhibitor depends on the nature of the metal, the mode of adsorption of the inhibitor and the surface conditions. Adsorption on C-steel surface is assumed to take place mainly through the active centers attached to the inhibitor and would depend on their charge density. Transfer of lone pairs of electrons on the nitrogen atoms to the C-steel surface to form a coordinate type of linkage is favored by the presence of a vacant orbital in iron atom of low energy. Polar character of substituents in the changing part of the inhibitor molecule seems to have a prominent effect on the electron charge density of the molecule. It was concluded that the mode of adsorption depends on the affinity of the metal towards the π -electron clouds of the ring system. Metals such as Cu and Fe, which have a greater affinity towards aromatic moieties, were found to adsorb benzene rings in a flat orientation. The order of decreasing the percentage inhibition efficiency of the investigated compounds in the corrosive solution was as follow: (1) > (2) and (3) > (4).

Compound (1) exhibits excellent inhibition power due to : (i) its larger molecular size that may facilitate better surface coverage, and (ii) the presence electron releasing groups (2N, 4O and 1S atoms) which enhance the

delocalized π -electrons on the active centers of the compound. Compound (2) comes after compound (1) in inhibition efficiency due to its lower molecular size than compound (1) and has 4O and 2N atoms as active centers. Compound (4) comes after compound (3) in inhibition efficiency due to its contain 2 Cl atom ., which lower the electron density on the molecule and hence, lower inhibition efficiency.

REFERENCES

- [1] M.A. Deyab, *Corros. Sci.* 49(2007) 2315-2328
- [2] S.A. Abd El-Maksoud A.S. Fouda, *Mater.Chem.phys.*93 (2005) 84-90
- [3] K.F.Khaled, *Mater. Chem.phys.* 122(2008) 290-300
- [4] E.Machnikova,K.H. Whitmire and N Hackeman, *Electrochim. Acta* 53(2008) 6024-6032
- [5] H Ashassi-sorkhabi, M.R. Magidi and K. Seyyedi, *Appl. Surf. Sci.*225 (2004)176-185
- [6] M.A. Migahed and I.F. Nasser, *Electrochim. Acta* 53 (2008) 2877- 2882
- [7] G.Avci, *Colloids Surf. A* 317 (2008)730-736
- [8] K.C.Pillali and R.Narayan, *Corros.Sci.* 23(1985)151
- [9] A.B.Tadros and B.A.Abdel-Naby, *J.Electroanal.Chem.*, 224(1988) 433.
- [10] JO'M.Bockris and B.Yang, *J.Electrochem.Soc.*, 138(1991) 2237.
- [11] V.Jovancicevic, B.Yang and JO'M.Bockris, *J.Electrochem.Soc.*, 135(1989) 94
- [12] J.Uhera and K.Aramaki, *J.Electrochem.Soc.*, 138(1991)3245.
- [13] A.A.Akust, W.J.Lorenz and F.Mansfeld, *Corros.Sci.* 22(1982) 611.
- [14] M. Abdallah, E. A. Helal and A. S. Fouda *Corros. Sci.*, 48 (2006) 1639-1654.
- [15] A. S. Fouda, A. A. Al-Sarawy and E. E. El-Katori. *Chem. Paper*, 60(1) (2006) 5-9.
- [16]A. S. Fouda, A. A. Al-Sarawy and E. E. El-Katori. *Desalination J.*, 201 (2006) 1-13.
- [17] O.Benali, L. Larabi, M Traisnel, L. Gengembra, Y. Harwk, *Appl. Surf. Sci* 253(2007)6130-6139.
- [18] M.A. Khalifa,M.El-Batouti, F.Mhgoub,A.Bakr Aknish, *Mater.Corrps.*54(2003)251-258.
- [19]Y.Abboud, A.Abourriche.T.Saffag,M.Berrada,M. Charrouf,A.Bennamara,N.Al Himidi and H. Hannache, *Mater. Chem.phy.*105 (2007) 1-5.
- [20] K.F Khaled, *Electrochim. Acta* 48 (2003)2493-2503
- [21] A. Popova M. Chistov, S. Raicheva and E. Sokolova, *Corros. Sci* 46(2004)1333-1350.
- [22] R.E. Khidre, A.A. Abu-Hashem, M. El-Shazly, *Eur. J. Med. Chem.*, 46(2011) 5057.
- [23] F. Bensajjay, S. Alehyen, M. El Achouri, S. Kertit, *Anti-Corros. Meth. Mater.* 50 (2003) 402.
- [24] S.Z. Duan, Y.L Tao, Interface Chem. Higher Education Press, Beijing, (1990)124.
- [25] S.S. Abd El-Rehim, S.A.M. Refaey, F. Taha, M.B. Saleh, R.A. Ahmed, *J. Appl. Electrochem.* 31 (2001) 429.
- [26] I.N.Putilova, S.A.Balezin, V.P.Barannik, *Metallic Corrosion Inhibitors*, Pergamon Press, New York, (1960) 31.
- [27].K.K. Al-Neami, A.K. Mohamed, I.M. Kenawy, A.S. Fouda, *Monatsh Chem.*, 126 (1995) 369.
- [28] E.A.Noor, *Int.J.Electrochem.Sci.*, 2(2007)996-1017.
- [29] J.Marsh, *Advanced Organic Chemistry*, 3rd ed,Wiley Eastern, New Delhi, (1988).
- [30] S.Martinez, *Appl.Surf.Sci.* 199(2002)83.
- [31]R.T.Vashi,V.A.Champaneri,*Indian J.Chem.Technol.* (1997)180.
- [32]A.K. Mohamed, H.A. Mostafa, G.Y. El-Awady, A.S. Fouda, *Port. Electrochim. Acta* 18 (2000) 99.
- [33] M. El Achouri, S. Kertit, H.M. Gouytaya, B. Nciri, Y. Bensouda, L. Perez, M.R. Infante and K. Elkacemi, *Prog. Org. Coat.*, 43 (2001) 267.
- [34] K.F. Khaled, *Electrochim. Acta*, 48 (2003) 2493.
- [35] F.B. Growcock and J.H. Jasinski, *J. Electrochem. Soc.*, 136 (1989) 2310.
- [36] U. Rammet and G. Reinhart, *Corros. Sci.*, 27 (1987) 373.
- [37] A.H. Mehaute and G. Grepy, *Solid State Ionics* 9–10 (1983) 17.
- [38] E. Machnikova, M. Pazderova, M. Bazzaoui and N. Hackerman, *Surf. Coat. Technol.*, 202 (2008) 1543.
- [39] C.H. Hsu and F. Mansfeld, *Corrosion* 57 (2001) 747.
- [40] M. Lebrini, M. Lagrenée, M. Traisnel, L. Gengembre, H. Vezin and F. Bentiss, *Appl. Surf. Sci.*, 253 (2007) 9267.
- [41] R.W. Bosch, J. Hubrecht,W.F. Bogaerts and B.C. Syrett, *Corrosion*, 57 (2001) 60.
- [42] Gamry Echem Analyst Manual (2003).
- [43] R.G. Kelly, J.R. Scully, D.W. Shoesmith and R.G. Buchheit, *Electrochemical Techniques in Corrosion Science and Engineering*, Marcel Dekker, Inc., New York, (2002) 148.
- [44] K. F. Khaled, *Int. J. Electrochem. Sci.* 3 (2008) 462.
- [45] K. F. Khaled, *Electrochim. Acta* 53 (2008) 3484.

- [46] D. A. Jones, Principles and Prevention of Corrosion, second ed., Prentice Hall, Upper Saddle River, NJ, (1983).
[47] R.A., Prabhu, T.V., Venkatesha, A.V., Shanbhag, G.M., Kulkarni, R.G., Kalkhambkar, *Corros.Sci.* 50 (2008) 3356
[48] G., Moretti, G., Quartanone, A., Tassan, A., Zingales, , *Wekst. Korros.*, 45(1994) 641
[49] C. Lee, W. Yang and R. G. Parr., *Phys. Rev. B*, 37 (1988) 785.
[50] R. M. Issa, M. K. Awad and F. M. Atlam, *Appl. Surf. Sci.*, 255 (2008) 2433